



# Prefunctionalised PLGA microparticles with dimethylaminoethyl moieties promote surface cell adhesion at physiological condition

Noelia D. Falcon<sup>\*</sup>, Aram Saeed<sup>\*</sup>

School of Pharmacy, University of East Anglia, Norwich NR4 7TJ, United Kingdom

## ARTICLE INFO

### Keywords:

Polyesters  
 Polylactic-co-glycolic acid (PLGA)  
 Cell adhesion  
 Microcarrier  
 Cell culture  
 Biomaterials  
 Adipose-derived stem cells  
 Cell therapy  
 Tissue engineering

## ABSTRACT

Synthetic hydrolytically degradable polyesters have seen widespread translation into a variety of clinical and biomedical settings; finding use as cell culture systems, drug delivery systems, tissue repair scaffolds, and medical devices. This success is owed in part due to their biocompatible nature and tuneable degradation profile. However, the lack of adhesion moieties limits the capacity of the polyesters to interact with cellular material and as such hampers their effectiveness within these applications. Several physical and chemical post-modification techniques have been developed to insert adhesion moieties; however, the nature of these methods remains complex and troublesome for translational medicine. To combat this flaw, we present a novel prefunctionalization method for the generation of poly (lactic-co-glycolic acid) PLGA microparticles with integrated adhesion moieties as a proof-of-principle. This strategy promotes surface cell adhesion at physiological conditions without the requirement for further post-modification. The basis of the prefunctionalization method was to utilise the 2-2-dimethylaminoethanol as an initiator in a standard bulk Ring Opening Polymerization process to obtain PLGA<sub>DMAE</sub> polymers. The resultant polymers were subsequently used in the fabrication of the microparticles, via membrane emulsion. This process allowed control over the morphology and size distribution of the microparticles. The surface cell adhesive properties of the new PLGA<sub>DMAE</sub> microparticles were investigated via co-culture with Adipose-Derived Stem Cells. Scanning Electron Microscopy showed that the new PLGA<sub>DMAE</sub> microparticles readily promote adhesion of the ADSCs at physiological conditions. LDH and LIVE/DEAD assays demonstrated that the surface functionalised PLGA<sub>DMAE</sub> microparticles maintained a low toxicity profile compared to the unmodified PLGA microparticles. Both thermogravimetric and differential scanning calorimetric analysis confirmed that the bulk properties of the polymer remained unchanged compared to the control PLGA. Gel Permeation Chromatography and Scanning Electron Microscopy imaging showed that the degradation profile of the new PLGA<sub>DMAE</sub> was enhanced compared to that of standard PLGA polymers. This novel prefunctionalization strategy eliminates the need for post-modification and could evolve rapidly to develop biodegradable biomaterials with enhanced cell adhesion and tuneable surface chemistry to allow greater control and/or maintain interaction with living cells and tissues. The implication of this new approach would be far reaching in the field of cell delivery, cell expansion, tissue engineering and regenerative medicine.

## 1. Introduction

Synthetic hydrolytically degradable polyesters such as poly (lactic acid) (PLA), poly (glycolic acid) (PGA), poly (lactic-co-glycolic acid) (PLGA), and poly(caprolactone) (PCL) are one of the most widely used polymers in the biomedical field, with applications including but not limited to cell culture systems, drug delivery systems, tissue repair scaffolds and medical devices [1–3]. The terminal functional groups such as ester and acid of polyester polymers play an important role in

modulating the degradation and release profiles of polyester polymers and have been widely used in the context of controlled drug delivery systems [4,5]. Their biologically inert nature and tuneable degradation profile coupled with their straight-forward and cost-effective production makes these polymers appealing both for research and commercial usage [6]. Microparticles (MPs) are one such usage of these polyester polymers [7]. Despite the success of the polyester and associated MPs, their applications in the development of more advanced tissue culture and cell delivery platforms have been hampered by their lack of cell

<sup>\*</sup> Corresponding author.

E-mail addresses: [N.Dominguez-Falcon@uea.ac.uk](mailto:N.Dominguez-Falcon@uea.ac.uk) (N.D. Falcon), [Aram.Saeed@uea.ac.uk](mailto:Aram.Saeed@uea.ac.uk) (A. Saeed).

<https://doi.org/10.1016/j.eurpolymj.2021.110466>

Received 11 March 2021; Received in revised form 7 April 2021; Accepted 13 April 2021

Available online 20 April 2021

0014-3057/© 2021 The Authors. Published by Elsevier Ltd. This is an open access article under the CC BY license (<http://creativecommons.org/licenses/by/4.0/>).

adhesion moieties, which is largely due to the hydrophobic surface of these polymers [8,9]. Consequently, the development of strategies to modify the surface of these polymers has garnered significant interest.

Several physical and chemical modification techniques have been established to address these issues. Examples of physical modifications included blending or surface coating of natural polymers containing cell adhesive sites (e.g., laminin, fibronectin, and vitronectin) [10–14]. In regard to chemical modifications, a popular strategy is the process of aminolysis to generate an active site on the polymer surface [15,16]. This site acts as a target for subsequent activation and conjugation with small molecules such as arginine-glycine-aspartic acid (RGD) peptides [17,18]. More recently, advanced surface-grafting of cationic polymers to a preformed polyester was reported using a specialist chain transfer molecule and living polymerization techniques [19–22]. Despite the progress in the development of post modification techniques the nature of these methods remains complex, challenging, and troublesome for translational medicine.

In this work we aimed to introduce a new and practical methodology for surface modification of polyester based materials that can readily promote cell adhesion at physiological conditions. We were particularly interested in strategies that allow the insertion of cell adhesion moieties such as small cationic functional groups into the structure of the polyester polymers in a one-step process. The rationale for using cationic groups was to enable interaction and adhesion with polyanionic cell membranes. In specific, we wanted to replace any post-functionalization methods.

Previous work by our group reported the prefunctionalization approach for surface modification of PCL MPs with azide functional groups, which were subsequently utilised for conjugation of a model protein via a copper-free click chemistry reaction at physiological conditions. This mechanism elicited a significantly higher and faster conjugation of the model protein on the surface of the prefunctionalised PCL MPs [23]. We decided to take this approach forward and so synthesised polyester polymers with cell adhesion moieties in the form of heterobifunctional tertiary amines.

To examine this method, we co-polymerised lactide and glycolic monomers from 2-dimethylaminoethanol (tertiary amine) (DMAEtOH) as an ROP initiator to generate a PLGA<sub>DMAE</sub> polymers with terminal dimethylaminoethyl (DMAE) groups. We chose the DMAEtOH since the pKa value of this tertiary amine is higher than that of physiological pH and expected to be positively charged, which in turn, may promote interaction with polyanionic cell membranes [24,25]. Subsequently, PLGA<sub>DMAE</sub> MPs were fabricated via membrane emulsion allowing relative control over the particle size and size distributions. In order to demonstrate the utility of the PLGA<sub>DMAE</sub> MPs for cell culture use, we targeted the MPs size to be equal to or >100 µm. This is approximately within the size range of commercially available MPs (namely micro-carriers) which are primarily used in suspension cell culture as a substrate for cell expansion purposes.

We analysed the PLGA<sub>DMAE</sub> MPs for surface adhesion with the clinically relevant cell type ADSCs and compared their performance against unmodified PLGA MPs under the same culture conditions. We rationalised that changing terminal functional groups may impact the bulk properties of the polymers. Therefore, we investigated the effect of the terminal DMAE groups on the degradation and cytotoxicity profiles of the newly synthesised PLGA<sub>DMAE</sub> polymers and compared it to that of the unmodified PLGA MPs. We also examined the macroscopic and molecular degradation of the new PLGA<sub>DMAE</sub> MPs under culture conditions, using GPC and SEM analyses. These studies were undertaken to demonstrate the advantage of prefunctionalization of PLGA<sub>DMAE</sub> polymers with terminal DMAE groups to promote cell adhesion without compromising the already attractive bulk properties, cytotoxicity, or degradation profiles of the PLGA polymer.

This new strategy of one-step prefunctionalization of polyester polymers, exemplified via PLGA<sub>DMAE</sub> synthesis using a standard bulk ROP process to introduce cell adhesion moieties, resulted in MPs with

surfaces that promote cell attachment at physiological conditions, which can be considered as a significant step forward. This new method can address the shortcomings, namely, the lack of cell adhesion, associated with the polyester polymers for advanced therapeutics and culture system applications.

## 2. Materials

Reagents were used as purchased, unless stated otherwise. Dimethylaminoethanol (DMAEtOH; ≥99.5%); citric acid (≥99.5); polyvinyl alcohol (PVA; Mw 13,000–23,000, 87–89% hydrolyzed); sodium chloride (NaCl; ≥99.5%); Hoechst 33,258 fluorescent dye; Paraformaldehyde were purchased from Sigma-Aldrich (UK). D, L-lactide (>98.0%), glycolide (>98.0%) and tin (II) 2-ethylhexanoate (>85.0%) were purchased from Tokyo chemical industry. Tetrahydrofuran (THF; ≥99.9%); dichloromethane (DCM; ≥99.5%); acetone (≥99.8%), methanol (≥99.8%); 2-propanol (≥99.7%) were purchased from VWR International. 1-Propanol (anhydrous, 99.9%) was purchased from Alfa Aesar™. Deuterated chloroform (CDCl<sub>3</sub>; ≥99.8%) was purchased from Acros Organics. Sodium hydroxide (NaOH; ≥99.0%) was purchased from Merck Millipore. Adipose tissue-derived stem cells (ADSCs), ADSCs basal media and supplements fetal bovine serum (FBS; 10%), L-glutamine (1%), gentamicin-amphotericin (0.1%); trypsin; trypsin neutralizing solution were purchased from Lonza. Phosphate Buffered Saline (PBS) tablets; trypan blue; were purchased from Thermo Fisher Scientific. CellTiter 96® Aqueous One Solution Cell Proliferation (MTS) Assay was purchased from Promega. CyQUANT™ Lactate dehydrogenase (LDH) Cytotoxicity Assay; LIVE/DEAD™ Viability/Cytotoxicity Kit, for mammalian cells were purchase from Thermo Fisher Scientific.

## 3. Methods

### 3.1. Synthesis of unmodified PLGA and PLGA<sub>DMAE</sub> Polymers

The PLGA<sub>DMAE</sub> polymer was synthesized via the standard bulk ring opening polymerization technique. First, a round bottom flask was degassed with nitrogen gas for 1 h into which the monomers D, L-lactide (11.3 g, 78.5 mmol), glycolide (9.1 g, 78.5 mmol) and the initiator 2-dimethylaminoethanol (0.1 g, 1.1 mmol, 117 µL) were added and the flask was tightly sealed with a septum. The mixture was then gradually heated to 140 °C under stirring and nitrogen conditions. Once the mixture was completely dissolved, the catalyst tin (II) 2-ethylhexanoate (0.046 g, 0.1 mmol) was added via a needle. The mixture was left to stir at the speed of 250 rpm and 140 °C for further 48 h. After this time, the reaction mixture was then cooled down and solidified polymer was collected from the flask. To directly compare the PLGA<sub>DMAE</sub> to unmodified PLGA, the latter was also synthesised under the same conditions except the DMAE was replaced with anhydrous 1-propanol as ROP initiator. A short oligo PLGA<sub>DMAE</sub> was also synthesized and purified, under the same condition, and characterised by <sup>1</sup>H NMR to elucidate the insertion of the DMAE group into the structure of the PLGA polymer. Samples from PLGA and PLGA<sub>DMAE</sub> polymers were collected for subsequent analyses.

### 3.2. Fabrication of PLGA and PLGA<sub>DMAE</sub> Microparticles

The PLGA and PLGA<sub>DMAE</sub> MPs were synthesised via the membrane emulsion technique, following a previously published protocol by our group using the Micropore LDC-1 dispersion kit (Micropore technologies, UK) [23]. Briefly, a continuous stabilizing solution was prepared by mixing PVA (20 g) and NaCl (26 g) in ultrapure water (1.8 L) under stirring and at 40 °C for overnight until complete dissolution. The solution was then vacuum filtered using a Buchner funnel. To this solution, 46 g of DCM solvent was gradually added and stirred for 1 h. The PLGA and PLGA<sub>DMAE</sub> (12.5% w/v) polymers were dissolved separately in DCM (14 mL) to produce the organic phase. To generate emulsion droplets,

the organic phase was injected via a stainless-steel hydrophilic ring membrane (40  $\mu\text{m}$  pore size) into the continuous phase (130 mL) at a rate of 0.50 mL/min, and preadjusted stirring speed of 600 rpm. The formed droplets were collected and transferred into a beaker. The mixture was then left to stir overnight under fume hood condition to evaporate the organic phase, resulting in the formation of solidified MPs. The MPs were then collected and transferred into a Buchner funnel and washed with ultrapure water several times to remove the residual of the PVA polymers. Finally, the MPs were collected via centrifugation at 1000 rpm for four minutes. The final MPs were freeze dried to obtain a loose dry powder and stored in a cold dry condition until further use.

### 3.3. Characterisation

The molecular weight of PLGA and PLGA<sub>DMAE</sub> were calculated using Gel Permeation Chromatography (GPC) analysis. The PL-GPC 50 was used in conjunction with a refractive index detector. A guard column (PLgel 5  $\mu\text{m}$  MiniMIX-C, 50/4.6 mm) was connected with two columns (PLgel 5  $\mu\text{m}$  Mixed-D, 300/7.5 mm) and maintained at 30 °C. The GPC machine was calibrated using Agilent EasiVial GPC poly methyl methacrylate calibration standards (PMMA; molar mass range:  $3 \times 10^5$ – $6 \times 10^5$  Da). To perform the analysis, a sample of PLGA and PLGA<sub>DMAE</sub> (approx. 1 mg/ml) was dissolved in THF solvent (HPLC grade) and injected at a flow rate of 1 mL/min. The data were collected and analyzed using CIRRUSTM data stream software.

<sup>1</sup>H NMR magnetic resonance spectroscopy was used to confirm the polymer structures, using the Bruker 400 MHz spectrometer. To do this, a small quantity of the PLGA and PLGA<sub>DMAE</sub> polymers were dissolved separately in deuterated chloroform (CDCl<sub>3</sub>; 1.2 mL) and <sup>1</sup>H NMR with average of 16 scans were recorded for each sample. The data was analysed using TopSpin<sup>TM</sup> NMR software v.4 and processed with MestReNova software v. 6.0.2–5475.

Thermogravimetric analysis (TGA) was performed on the PLGA and PLGA<sub>DMAE</sub> polymers. Approximately 1–5 mg of the polymers were placed in tared unsealed standard aluminium pans (TA instruments). The data was recorded under nitrogen atmosphere and analyzed using a TGA 5500 analyzer (TA Instruments). The samples were heated from room temperature to 400 °C and at heating a rate of 10 °C/min. Two set of data were collected including weight loss (%) profile and derivative weight (%/°C) as a function of temperature. All measurements were recorded using TRIOS software.

Differential Scanning Calorimetry (DSC) analysis was performed on the polymers to determine the glass transition temperature ( $T_g$ ). Approx. 1–5 mg of the polymers were placed in sealed standard aluminium pans (TA instruments), and an empty sealed standard aluminium pan (TA instruments) was used as a reference. The data was collected using a DSC 2500 analyser (TA Instruments) and under nitrogen atmosphere. To do this, the samples were equilibrated first at –10 °C, and then heated to 150 °C at a rate of 10 °C/min, then cooled to –10 °C at a rate of 10 °C/min. Finally, the samples were heated again to 150 °C at the same heating rate of 10 °C/min (to obtain three cycles in total). The  $T_g$  of the polymers were obtained from the second heating event to remove any interference from the residual moisture in the samples. A heat flow measurement (W/g) as a function of increasing temperature profile were then obtained. All measurements were recorded using TRIOS software.

### 3.4. Microparticle size and size distribution analysis

The mean particle size and particle size distributions for PLGA and PLGA<sub>DMAE</sub> MPs were measured using optical EVOS XL Core phase contrast microscope (Thermo Fisher Scientific). To calculate the span, the average diameter (D) in  $\mu\text{m}$  of solidified microparticles was calculated from circular 2D optical surface area using the oval tool from ImageJ software. This tool was used to select the circumference of the particles. 20 representative images of PLGA and PLGA<sub>DMAE</sub> MPs were taken at 20X magnification, and a minimum of 40 particles per image

were used for data analysis. Span was then calculated from the D10, D50 and D90 corresponding to the diameters at 10, 50 and 90 percentiles, respectively. The D90 were subtracted from D10 values and the result was then divided by D50. Distribution histograms were created with SPSS statistical software (IBM Corp. Released 2020. IBM SPSS Statistics for Windows, Version 27.0. Armonk, NY: IBM Corp) to illustrate the dispersity of MPs.

The morphology of the MPs was also analysed by Scanning Electron Microscopy (SEM) imaging. Briefly, freeze dried MPs were loaded onto the aluminium stubs with carbon tabs and then gold coated with a Quorum Technologies Polaron Gold Sputter Coater (rotary stage, 30sec, 20 mA, 2.2 kV, average distance from Au target: 55 mm). The MPs were then imaged using a Zeiss Gemini SEM 300 at an accelerating voltage of 2 kV.

To investigate if the UV sterilization process had any impact on structure and morphology of the MPs, confirmatory (<sup>1</sup>H NMR) and SEM analyses were performed on the MPs before and after UV sterilization process. The samples were analyzed following the protocol described earlier for each technique. To further supplement the analysis, Fourier-Transform Infrared Spectroscopy (FT-IR) was conducted on the PLGA and PLGA<sub>DMAE</sub> MPs before and after UV irradiation. FT-IR spectra were recorded on a Bruker Vertex 70 V FTIR Spectrometer equipped with Golden Gate<sup>TM</sup> Heat-enabled ATR accessory (Specac LTD, UK) in absorption mode against wavenumber. The OPUS software was used to record the spectra at 4  $\text{cm}^{-1}$  resolution using 32 scans. The wavenumber range of the spectra was selected from 550 to 4000  $\text{cm}^{-1}$ .

### 3.5. Cell culture

Human Adipose-Derived Stem cells (ADSCs) (PT-5006, Lot number 0000439846) were purchased from Lonza (statement from the supplier confirm the cells were obtained under ethical conditions with the donor consent and tissue acquisition letter is available upon request). Cells were received in passage one, expanded to passage three using monolayer culture condition following the manufacturer protocols (Catalogue number PT-4505; Lonza). Cells were cultured in ADSCs Basal Media (supplemented with 10% FBS, 1% of L-glutamine, and 0.1% of gentamicin amphotericin) and maintained in humidified atmosphere with 5% CO<sub>2</sub> in the air at 37 °C prior to the experiments.

### 3.6. Cell attachment

The freeze dried PLGA and PLGA<sub>DMAE</sub> MPs were sterilised by standard UV irradiation (for 1.5 h). The MPs powder was loaded into a glass vial and rotated on a laboratory roller to maximise the light exposure. The sterilised MPs were prepared in cultured condition. Briefly, 10 mg of the freeze-dried MPs were resuspended in 1 mL of the complete cell culture media for 12 h at room temperature. Following this step, the media was removed from the MPs suspension via centrifugation at 1000 rpm for four minutes followed by gentle aspiration of the supernatant, leaving the conditioned MPs in place.

Two methods were followed to study the cell attachment to the MPs. In (Method 1), 20,000 cells suspended in 250  $\mu\text{L}$  complete media were mixed with 10 mg of the MPs to obtain a final concentration of  $2 \times 10^3$  cells·mg<sup>-1</sup> of MPs (the calculated surface area of the MPs equals to 0.4  $\text{cm}^2$ ·mg<sup>-1</sup>). This mixture was directly transferred into the well of a 24-well cell culture plate and topped up to 1 mL with cell culture media. In (Method 2), we followed an in house developed protocol to maximise cell attachment by mixing the MPs and cells in closer proximity. Cells and MPs were mixed using the same concentrations as before. From this mixture, 20  $\mu\text{L}$  of the cells and MPs mixture were pipetted (wide orifice pipette tips were used) onto an inverted lid of a 60 mm diameter petri dish, which was gently flipped over and placed on top of the petri dish containing 5 mL of PBS in order to maintain a humidified environment. Following 24 h incubation and under the described conditions, all the droplets collected from each Petri dish lid were transferred into one well

of a 24-well tissue culture plate, which was previously filled with 500  $\mu\text{L}$  of cell culture media. After the transfer of the droplets, each well was topped up to 1 mL with complete media. The mixture of cells and MPs was maintained in a humidified atmosphere with 5%  $\text{CO}_2$  and 37  $^\circ\text{C}$  for predetermined time intervals. All experiments were conducted in static conditions and the cell culture media was refreshed every three days (approximately, 600  $\mu\text{L}$  of cell culture media was gently removed and replaced by fresh media).

### 3.7. Cytotoxicity study

ADSCs were cultured on PLGA and PLGA<sub>DMAE</sub> MPs, as previously described (method 2), in 24-well cell culture plates for 1, 5, 7, and 14 days, and the LDH analysis was performed following the manufacturer's instructions. Briefly, 50  $\mu\text{L}$  of cell culture media was withdrawn from tissue culture plates and mixed with CyQUANT™ LDH Cytotoxicity Assay Kit LDH reagent in a 1:1 ratio. Following 30 min incubation at room temperature and storage in a dark place, LDH stop solution was added. The absorbance values were measured at 490 and 680 nm with a microplate reader (CLARIOSTAR; BMG Labtech). Background absorbance at 680 nm was subtracted from the 490 nm absorbance. Cell culture media without cells was used as a blank.

Phase contrast microscopy was used to monitor all cell culture conditions. Representative images were taken 1, 5, 7 and 14 days after culture using an EVOS XL Core (Thermo Fisher Scientific) phase contrast microscope. Images were taken with 10X or 20X magnification and processed using ImageJ software.

### 3.8. Live/Dead assay

ADSCs were cultured on PLGA and PLGA<sub>DMAE</sub> MPs in 24-well cell culture plates (method 2) for 1, 7, and 14 days. Approximately, 600  $\mu\text{L}$  of media was removed from the culture dishes and MPs were washed once with 600  $\mu\text{L}$  of PBS. Then, the PBS was gently removed. Freshly prepared Calcein AM and Ethidium homodimer-1 solution (2 and 4  $\mu\text{M}$ , respectively) was prepared following manufacturer's instructions, added to the cells and MPs mixture, and incubated for 40 min in the dark at room temperature. Next, imaging was performed using a Zeiss Axiovert 200 M microscope using Axiovision software. Images were taken with a 20x magnification Plan-Neofluar (NA 0.5) objectives and a Zeiss AxioCam HRm CCD camera. Fluorescence was excited either at 494–517 nm (Calcein) or 528–617 nm (Ethidium homodimer-1). Merged images of Calcein (green), Ethidium homodimer-1 (red) and Bright Field were created in Image J software. Live and Dead cells were counted in every picture, using a minimum of three random locations per sample.

### 3.9. Cell attachment analysis

SEM imaging was used to investigate cell attachment onto the PLGA and PLGA<sub>DMAE</sub> MPs. The ADSCs were cultured on PLGA and PLGA<sub>DMAE</sub> MPs, as previously described in 24-well cell culture plates (method 2) for 7 days (this was considered a midpoint between start of the culture and sufficient cell attachment and growth). Approximately, 600  $\mu\text{L}$  of media was removed, and the remaining cells and MPs mixture were fixed with freshly prepared 4% paraformaldehyde in PBS for 30 min at room temperature. Fixed cells and MPs mixture were washed three times with PBS and centrifuged at 1000 rpm for four minutes, which were collected and freeze dried. The freeze dried powder was loaded onto aluminium stubs with carbon tabs. The samples were gold coated with a Quorum Technologies Polaron Gold Sputter Coater (rotary stage, 30sec, 20 mA, 2.2 kV, average distance from Au target: 55 mm) and subsequently imaged using a JSM 5900LV (JEOL) SEM at an accelerating voltage of ~10 kV.

### 3.10. Degradation study

PLGA and PLGA<sub>DMAE</sub> MPs were prepared as previously described. The MPs were immersed in 2 mL of PBS, incubated at 37  $^\circ\text{C}$  in a water bath for 7, 14, and 21 days, and samples were collected and freeze dried.

First, the macroscopic and morphological changes were studied using SEM, samples were prepared following the same protocol as described earlier. SEM images of the MPs were acquired using a Zeiss Gemini SEM 300 at an accelerating voltage of 2 kV.

Secondly, the molecular degradation of the MPs was examined using GPC. The freeze dried MPs were dissolved in 2 mL of THF (HPLC grade) for 24 h at room temperature. After complete dissolution, the samples were injected and analysed using the previously described protocol. The shifting in the number-average molecular weight ( $M_n$ ) of the PLGA and PLGA<sub>DMAE</sub> MPs were analyzed and compared to that of the undegraded polymers.

### 3.11. Statistical analysis

For the particle size and particle size distribution, frequency distribution histograms were created with SPSS statistical software to illustrate the dispersity of microparticle diameter with associated Span values. A bar chart was plotted to compare the mean particle size between PLGA and PLGA<sub>DMAE</sub> MPs representing the mean particle size ( $\mu\text{m}$ )  $\pm$  SD ( $n = 20$  representative images of PLGA and PLGA<sub>DMAE</sub> MPs). A two-tailed unpaired *t*-test was used to assess significant differences between the particle size of both groups. ns: non-significant. In regard to the cytotoxicity study using the LDH assay, the data are presented as optical density values (OD)  $\pm$  SD ( $n = 3$  independent cell culture replicates). Differences between groups were assessed via a two-way ANOVA with a Tukey's multiple comparison test. Ns: non-significant, \*  $p = 0.03$ , \*\*\* $p < 0.0002$ , \*\*\*\* $p < 0.0001$ . In the Live/Dead staining experiment, data are presented as the average of counted cells per field  $\pm$  SD ( $n = 3$  independent technical cell culture replicates) in three random locations, therefore using a total of 9 images per sample. Ns: non-significant.

## 4. Results and discussion

The overarching aim of this work was to address the lack of cell adhesion in hydrolytically degradable polyester polymers. It is known that the presence of cationic functional groups in the structure of synthetic materials can facilitate interaction with polyanionic cell membranes [26,27]. Therefore, we set out to insert cationic functional groups into the terminal end of these polymers via the ROP technique. To achieve this strategy, we chose to use 2-dimethylaminoethanol (DMAEtOH) as a heterobifunctional initiator. The hydroxyl group of DMAEtOH was used to initiate the ROP of the polymers to insert tertiary amine groups. We hypothesised that tertiary amine groups on the terminal end of the synthesised polymers would become protonated at physiological conditions and thus can display positive charges to interact with cell membranes. We compared this new polymer to a standard PLGA polymer (control) synthesised under the same condition but with 1-propanol as the initiator (Fig. 1 A).

The theoretical feeding ratio and ROP polymerization conditions for both PLGA and PLGA<sub>DMAE</sub> polymers are summarised in (Table 1). The GPC analysis showed that the number-average molecular weight ( $M_n$ ) and polydispersity (PDI) of both PLGA and PLGA<sub>DMAE</sub> polymers were comparable as measured against the PMMA standards (See Fig. S1 A-B, Supporting Information (SI)). The  $M_n$  for the PLGA<sub>DMAE</sub> measured was 26,400 Da with PDI ( $\text{Đ}$ )<sub>m</sub> 1.6 and a yield of > 90%, compared to that of the PLGA polymer with an  $M_n$  of 26,563 Da with PDI ( $\text{Đ}$ )<sub>m</sub> 1.6 and also a yield of >90% (Table 1).

Next, the chemical structures of the PLGA and PLGA<sub>DMAE</sub> polymers were confirmed by  $^1\text{H}$  NMR analysis. The spectra for both polymers confirmed the main structure and peaks for the repeating monomer units

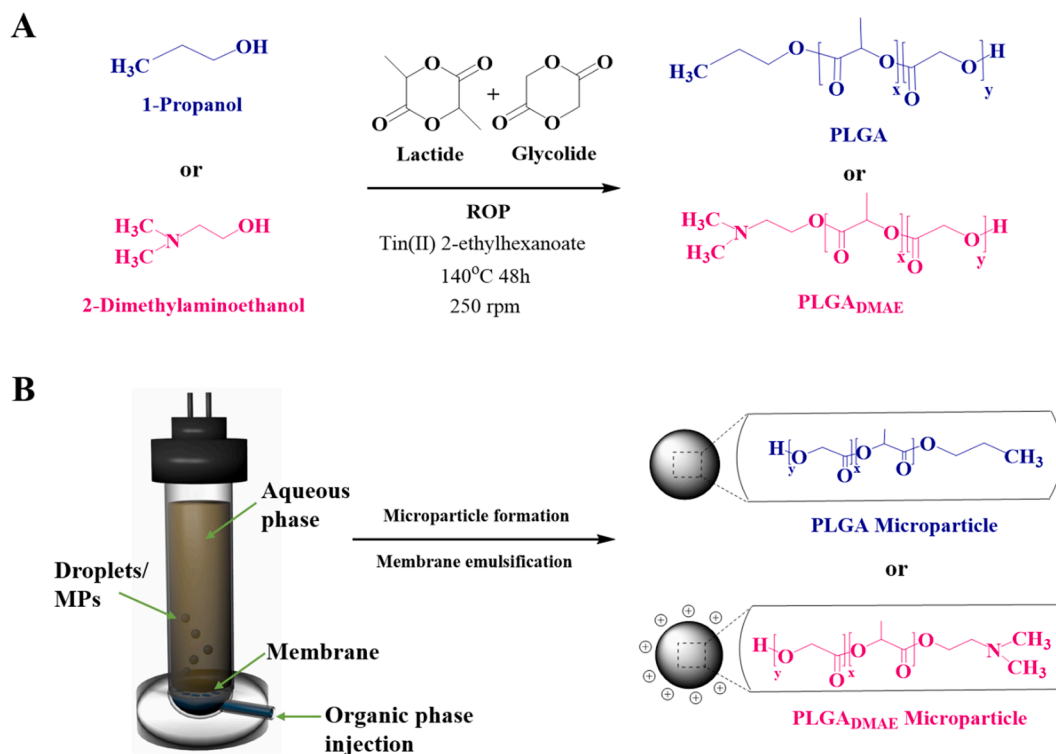


**Fig. 1.** Schematic illustration of the one step synthesis and fabrication of the prefunctionalised PLGA<sub>DMAE</sub> MPs versus the control PLGA MPs. (A) Standard ROP of the D, L Lactide and Glycolide monomers, using Tin (II) as catalyst and heating at 140 °C for 48 h under nitrogen condition. (B) Fabrication of PLGA or PLGA<sub>DMAE</sub> MPs via the membrane emulsification process.

**Table 1**

PLGA and PLGA<sub>DMAE</sub> synthesis feed ratio (mol%), relative molecular weight ( $\text{g}\cdot\text{mol}^{-1}$ ), polydispersity and yield (%) as measured by GPC analysis and using PMMA as standards.

Polymer	Theoretical Feed ratio (mol %)			Relative molecular weight ( $\text{g}/\text{mol}$ )		Dispersity	Yield (%)
	Lactide	Glycolide	Initiator	Mn	Mw		
PLGA	71	71	1	26,563	42,980	1.6	>90
PLGA <sub>DMAE</sub>	71	71	1	26,400	41,381	1.6	>90

of lactic acid and glycolic acid. We calculated the composition to confirm the 50/50 ratio, which was measured by integrating the peaks of the two repeating units. The  $^1\text{H}$  NMR spectra of both polymers showed the typical peak characteristics for the monomers with chemical shifts detected at 5.2 ppm (CH, 1H) and 1.6 ppm (CH<sub>3</sub>, 3H) for lactic acid, and at 4.8 ppm (CH<sub>2</sub>, 2H). for glycolic acid. A short oligo PLGA<sub>DMAE</sub> was also synthesized and its structure was confirmed by  $^1\text{H}$  NMR showing the successful initiation of the PLGA polymer from the DMAE initiator, (See Fig. S2, Supporting Information (SI)).

Next, the thermal properties of the polymers were analyzed using both thermogravimetric (TGA) and differential scanning calorimetry (DSC) to investigate whether the insertion of the new DMAE terminal functional groups affects the physicochemical properties of the new prefunctionalised PLGA<sub>DMAE</sub> polymer. As can be seen in (Fig. S3 A, SI), there was a 50% weight reduction at 287 °C and 285 °C for PLGA and PLGA<sub>DMAE</sub>, respectively. The derivative weight supported these findings; demonstrating that the maximum rate of degradation temperature (MRDT) between the two polymers were likewise similar.

A similar observation was also recorded from the DSC analysis which was used to determine the glass transition temperature ( $T_g$ ) of the two polymers (Fig. S3 B, SI). The results showed that both polymers possess a similar  $T_g$  at 44 °C, this value is broadly similar to the reported  $T_g$  for PLGA polymers having 50:50 ratio of composition of lactic acid to glycolic acid units [28]. These analyses confirmed that the thermal profiles

were comparable with negligible differences between the two polymers.

In the next step, MPs were fabricated via the single oil-in-water membrane emulsion technique (Fig. 1 B). We targeted the diameter of the MPs to be equal to or >100  $\mu\text{m}$ . The rationale behind this was that the range is relatively close to that of commercially available MPs, which are used as a cell culture substrate in suspension cell culture systems.

The PLGA and PLGA<sub>DMAE</sub> MPs were both prepared under the same emulsification parameters and polymer concentrations. Preliminary work (data not shown) suggested that a polymer concentration of 12.5% w/v (adjustable based on the polymer molecular weight) was sufficient to achieve MPs within the target size range. Under the described conditions (see the method section), MPs were successfully fabricated from both polymers. The comparative size and morphology of fresh droplets, solidified MPs, and freeze dried MPs derived from the PLGA and PLGA<sub>DMAE</sub> polymers were assessed using phase contrast microscopy (Fig. 2, A) and SEM imaging (Fig. 2, B). The phase contrast and SEM imaging confirmed the successful formation of spherical MP morphologies. Further analysis of the phase contrast images demonstrated that the distribution of the particle sizes was unimodal and possessed little variance (Fig. 2, C), suggesting near uniform particle sizes distribution for both PLGA and PLGA<sub>DMAE</sub> MPs. The calculated Span values from the phase contrast imaging were also compared between the PLGA and PLGA<sub>DMAE</sub> MPs which showed a value of 0.3 suggesting a narrow particle size distribution. Furthermore, the mean particle size and relative

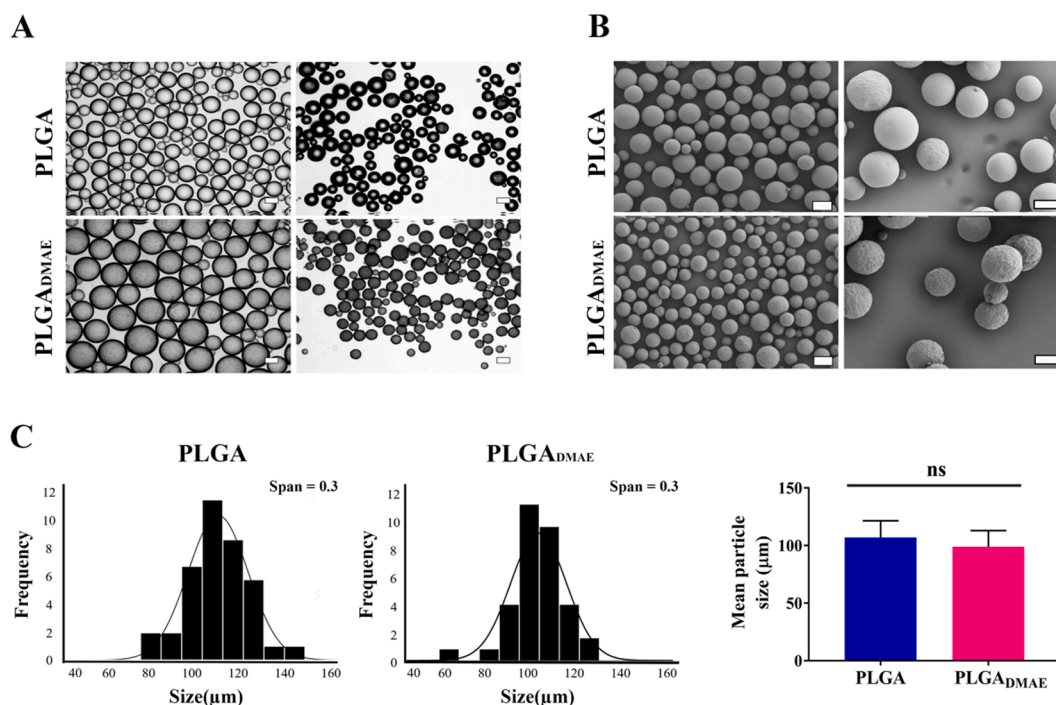


**Fig. 2.** There are no significant differences in the morphologies or size distribution between the PLGA and PLGA<sub>DMAE</sub> Microparticles. (A) Phase Contrast imaging of freshly prepared (left) and solidified (right) PLGA and PLGA<sub>DMAE</sub> microparticles. Scale bar is 100  $\mu\text{m}$  (10 $\times$  magnification). (B) SEM of freeze dried PLGA and PLGA<sub>DMAE</sub> microparticles. Scale bar is 100  $\mu\text{m}$ . (C) Frequency histograms, Span values and accompanying information regarding the size distribution and mean particle size comparison of PLGA and PLGA<sub>DMAE</sub> microparticles. Mean particle size comparison between PLGA and PLGA<sub>DMAE</sub> microparticles is shown as bar charts. Data is presented as mean particle size ( $\mu\text{m}$ )  $\pm$  SD ( $n = 20$  representative images). A two-tailed unpaired  $t$ -test statistical analysis was applied. Ns: non-significant.

standard deviation were also plotted as bar charts in (Fig. 2, C), indicating that there was no significant difference between the two MP groups. These data suggest that the prefunctionalised polymer did not alter the size or the morphology of the MPs.

With the uniformity of the MP size and morphology between the two polymers established, we next sought to address whether the surface functionalization affected the cytotoxicity profiles. Prior to the cytotoxicity assays, the morphology and chemical properties of the PLGA and PLGA<sub>DMAE</sub> microparticles were investigated before and after UV sterilization, using SEM imaging, FT-IR and  $^1\text{H}$  NMR. The results confirmed that no changes occurred as a result of the sterilization (Fig S4, SI).

Two methods were investigated to evaluate the efficiency of seeding ADSCs onto the MPs. In (Method 1) followed a standard protocol by mixing cells with the MPs in the 24-well plate tissue culture plastic [29] whereas in (Method 2), cells were mixed with MPs in form of hanging droplets for 24 h to enhance the exposure of the cells to the MPs in closer proximity. As can be seen in (Fig. S5, SI), the nuclei staining and phase contrast imaging suggested that the aggregation of the ADSCs with the MPs were significantly higher in (Method 2) compared to that of (Method 1). Therefore, we have followed method 2 for the rest of the work.

We performed the cytotoxicity study on the MPs co-cultured with ADSCs, using LDH and LIVE/DEAD assays, and the results were analyzed at day 1, 5, 7 and 14 post culture. The absorbance value of Formazan (directly proportional to the amount of LDH released into the medium) was recorded as function of time post culture. In (Fig. 3, A), we detected a significantly lower concentration of LDH released into the medium of the PLGA<sub>DMAE</sub> MPs group at day 1 post culture, compared to that of the PLGA, which infers a higher survival rate. At this point, the differences observed in the LDH concentration between the two group was probably due to the differential attachment of the ADSCs to the PLGA and PLGA<sub>DMAE</sub> MPs within the first 24 h. However, the differences in LDH concentrations observed between the two groups at day 5, 7 and 14 post

culture were not statistically significant, which was probably because the remaining cells were either adhered to the surface of the PLGA<sub>DMAE</sub> MPs or to the surface of the tissue culture plastic when co-cultured with the unmodified PLGA MPs. This was supported by the fact that the phase contrast imaging showed that the ADSCs were attached to the PLGA<sub>DMAE</sub> MPs, whereas in the unmodified PLGA MPs group, cells were mostly adhered to the tissue culture plastic (Fig S6, SI).

Taken together, these data suggest that following the successful attachment and survival advantage in the first 24 h period, the PLGA<sub>DMAE</sub> MPs maintained the already desirable low toxicity profile of PLGA polymers. Furthermore, the LIVE/DEAD viability assay indicated that there was no significant difference to the viability of the cells co-cultured with either PLGA<sub>DMAE</sub> or PLGA MPs over the cultured time period (Fig. 3, B-C).

Although the previous assays showed that the PLGA<sub>DMAE</sub> MPs were well tolerated when co-cultured with the ADSCs, more investigations were required to show that cells can attach to the surface of the PLGA<sub>DMAE</sub> MPs at physiological conditions. Thus, ADSCs were co-cultured with PLGA and PLGA<sub>DMAE</sub> MPs for 7 days and surface cell attachments were investigated using SEM imaging (Fig. 4). A pilot study (data not shown) demonstrated that day 7 was the most appropriate timepoint to image the attachment of the ADSCs to the MPs as it represented a midpoint between early cell attachment and over confluent cell culture conditions. It was strongly evident from the analysis that the PLGA<sub>DMAE</sub> MPs readily attached to the co-cultured ADSCs, (Fig. 4, bottom row), compared to no or poor attachment of the ADSCs to the PLGA MPs (Fig. 4, top row). Once again, the SEM imaging suggested that the ADSCs were predominantly attached to the tissue culture plastic when using PLGA MPs (Fig. 4, bottom row).

In addition, the ADSCs attached to the PLGA<sub>DMAE</sub> MPs had different morphologies compared to those co-cultured with the PLGA MPs. Cells attached to the PLGA<sub>DMAE</sub> MPs adopted elongated morphologies; gripping and spreading across the different MPs surfaces, which suggested the presence of a strong interaction at the interface between the MPs and

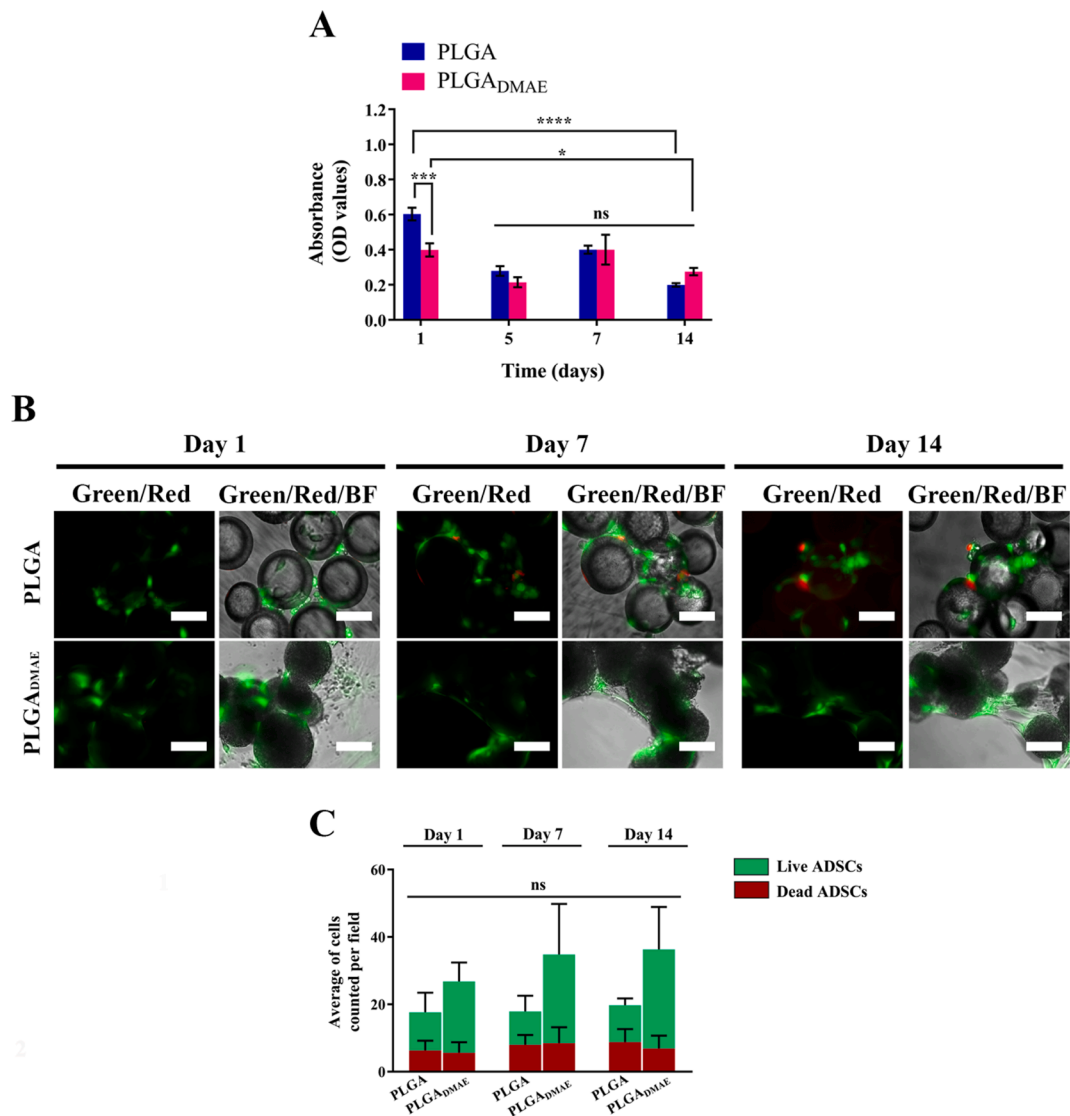


**Fig. 3.** PLGA<sub>DMAE</sub> microparticles retain a low cytotoxicity profile and is comparable to non-functionalised PLGA microparticles. (A) LDH assay performed on ADSCs in the presence of PLGA or PLGA<sub>DMAE</sub> MPs, analysed at days: 1,5,7, and 14 post-culture. Data are presented as optical density values (OD) ± SD (n = 3 independent cell culture replicates). Differences between groups were assessed via a two-way ANOVA with a Tukey’s multiple comparison test. Ns: non-significant, \* p = 0.03, \*\*\*p < 0.0002, \*\*\*\*p < 0.0001. (B) Representative fluorescent images showing the LIVE (Calcein AM- green)/DEAD (ethidium homodimer-1- red) staining of the co-cultured cells with the MPs at different time intervals. Scale bar is 100 μm (20X magnification). (C) Average number of cells per field of view that were classified as either alive or dead. Data are presented as the average of counted cells per field ± SD (n = 3 independent technical cell culture replicates) in three random locations, therefore using a total of 9 images per sample. Ns: non-significant.

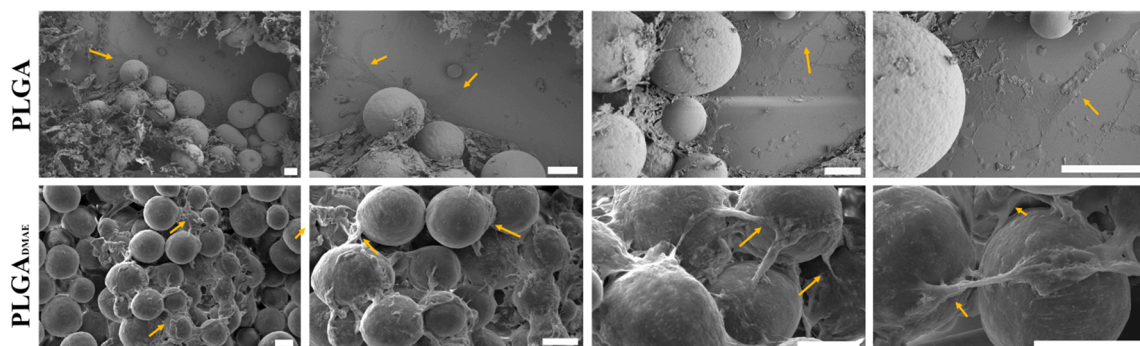


**Fig. 4.** ADSCs readily adhere to PLGA<sub>DMAE</sub> microparticles and show differential cellular morphologies when compared to ADSCs co-cultured with unmodified PLGA microparticles. Representative SEM images of ADSCs co-cultured with PLGA microparticles (top) or PLGA<sub>DMAE</sub> microparticles (bottom). All scale bars are 100 μm.

cells (Fig. 4, bottom row). On the other hand, the cells co-cultured with the unmodified PLGA MPs were attached to the tissue culture plastic and displayed typical 2D monolayer flat morphologies (Fig. 4, top row).

Therefore, we postulated that the cell attachment to the surface of the PLGA<sub>DMAE</sub> MPs was most probably due to the presence of a weak electrostatic interaction between the positively charged DMAE functional groups available on the surface of the PLGA<sub>DMAE</sub> MPs and the polyanionic cell membranes. The lack of any cell adhesion moieties on the unmodified PLGA MPs resulted in poor or no cell adhesion. This confirms the hypothesis that the PLGA<sub>DMAE</sub> MPs readily promoted the attachment of the clinically relevant ADSCs at physiological condition.

Next, to evaluate the degradation profile and morphology of the PLGA and PLGA<sub>DMAE</sub> MPs, we resuspended the MPs in PBS (pH 7.4 and at 37 °C) and samples were taken for analysis at days 7, 14, and 21 post incubation. First, SEM imaging was used to observe the changes to the morphology of the MPs, namely changes that occur due to surface and

bulk erosion. To demonstrate these changes to the surface and bulk of the MPs, SEM images were taken at low and high magnifications, respectively. In addition, GPC profiles were also monitored to characterize the changes to the molecular weight and molecular weight distributions. As shown in (Fig. 5, A), on day 7 of incubation, the morphologies of the PLGA and PLGA<sub>DMAE</sub> MPs were broadly similar. However, SEM images taken on day 14 and 21 showed the appearance of deformation and coalescence in the structures of PLGA<sub>DMAE</sub> MPs. Concomitant with this was presence of larger pore sizes across the surfaces and bulk of the MPs, indicating ongoing surface degradation. In contrast, the PLGA MPs preserved their spherical morphologies at day 14 and 21 but showed early signs of surface erosion indicated by the appearance of surface cracking. However, no sign of bulk erosion among the PLGA MPs was observed.

The recorded GPC profiles for the samples analyzed from the cultured PLGA MPs, (Fig. 5, Bi), showed a shift in the molecular weight

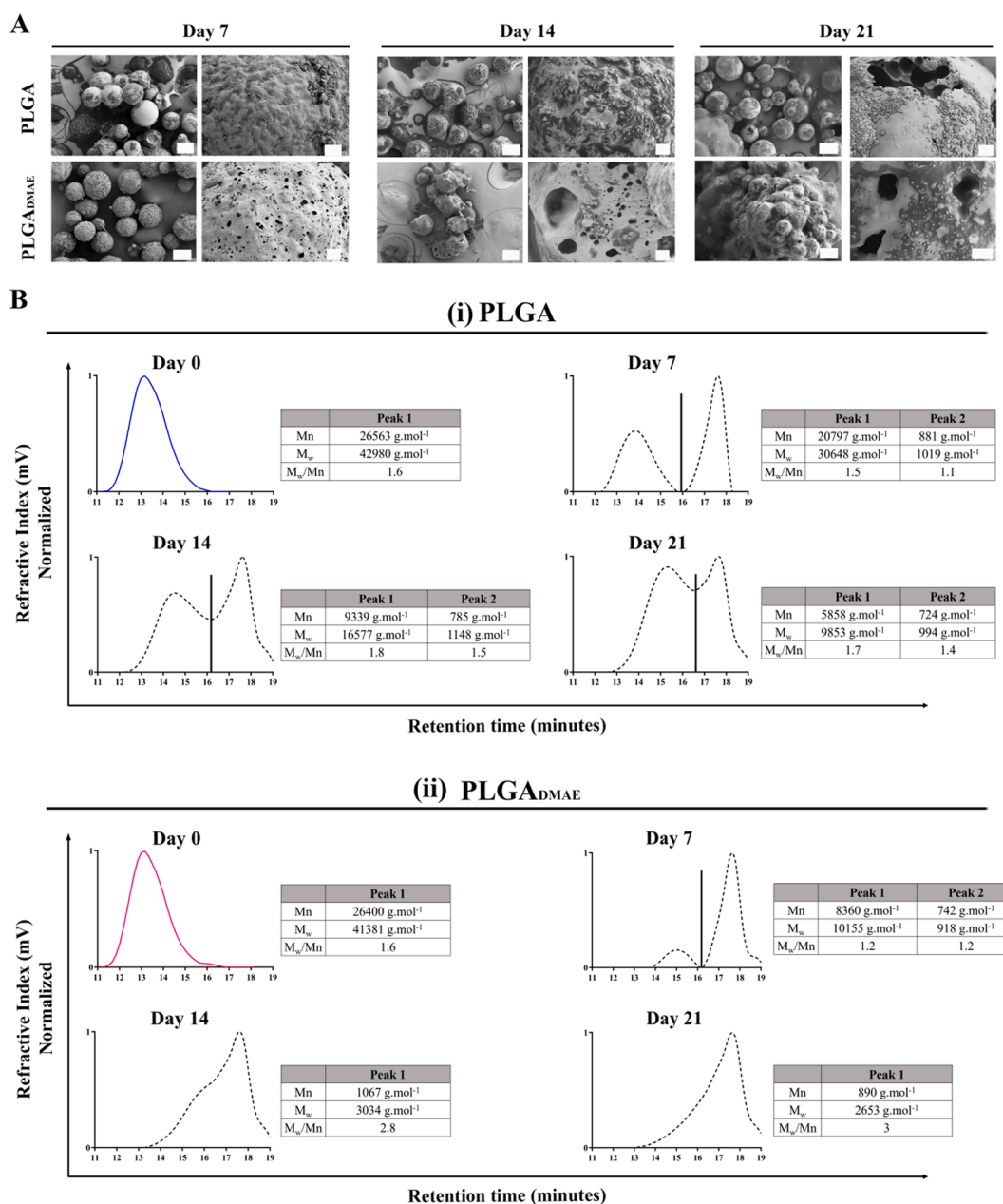


**Fig. 5.** PLGA<sub>DMAE</sub> microparticles degrade more rapidly and uniformly than unmodified PLGA microparticles. (A) SEM of PLGA and PLGA<sub>DMAE</sub> microparticles immersed in PBS at 37 °C at days 7, 14, and 21 after incubation. Scale bars are 100 μm (high magnification) or 10 μm (low magnification). (B) Normalised GPC chromatograms, recorded with Refractive Index detector, depicting the shift in the molecular weight over time for (i) PLGA and (ii) PLGA<sub>DMAE</sub> MPs.

from a unimodal (at day 0) to a bimodal (at day 7, 14 and 21) distribution, suggesting a slow and partial reduction in the molecular weight from a higher to a lower range. However, the GPC profile for the PLGA<sub>DMAE</sub> MPs showed faster and more uniform degradation as depicted by the persistence of a unimodal distribution throughout the study (Fig. 5, Bii). This was also supported by the calculated number average molecular weight values that showed a faster reduction in the molecular weight of the PLGA<sub>DMAE</sub> compared to that of the PLGA MPs.

The differences observed in the macroscopic and molecular degradation profiles between PLGA and PLGA<sub>DMAE</sub> MPs were expected. This is because there are many reported factors that can affect the hydrolytic degradation of the polyester polymers, including polymer structure, molecular weight, crystallinity, as well as hydrophilicity of the terminal functional groups, which is more relevant to this work [30–32]. Therefore, we postulated that the insertion of the hydrophilic DMAE groups into the terminal structure of the PLGA polymers was responsible for enhanced molecular degradation of the PLGA<sub>DMAE</sub> polymer compared to that of the unmodified PLGA. Similarly, the morphological changes observed with the PLGA<sub>DMAE</sub> MPs were most likely due to enhanced water diffusion and thus increased accessibility of water molecules to weak and hydrolytically labile ester bonds. Nonetheless, the overall benefit of faster degradation of the PLGA<sub>DMAE</sub> MPs compared to unmodified PLGA may depend on the end application, which may require further evaluation.

Taken together, this study presents a simple one-step strategy to prefunctionalise polyester polymers so to produce biomaterials with enhanced cell surface attachments at physiological conditions. This strategy also eliminates the requirement for laborious and extensive post-functionalization processes. The PLGA<sub>DMAE</sub> MPs presented in this work readily attached to the clinically relevant cell type, ADSCs, maintained low toxicity and displayed more uniform degradation profiles compared to PLGA.

## 5. Conclusions

In this work, we introduced a new strategy to prefunctionalise hydrolytically degradable polyester polymers with cell adhesive moieties to address the shortcoming of these polymers intended for advanced biomedical applications. We validated the prefunctionalization method by synthesizing PLGA polymers with DMAE groups using a standard ROP technique. The introduction of the DMAE groups into the PLGA polymers did not change the bulk or thermal properties of the polymers. We also demonstrated the successful fabrication of MPs via a membrane emulsion technique. Furthermore, we showed that the clinically relevant ADSCs more readily attach to the surface of these MPs at physiological conditions, compared to no or poor attached unmodified PLGA MPs. We also assessed the impact of the prefunctionalization strategy on the degradation profile of the polymers. The introduction of the DMAE group elicited a faster and more uniform degradation of the PLGA<sub>DMAE</sub> polymer. Importantly, we demonstrated that PLGA<sub>DMAE</sub> MPs maintained the already desirable low cytotoxicity profile associated with PLGA MPs. This data set validates the prefunctionalization strategy and could be widely used to develop other hydrolytically degradable polyesters with a broad range of advanced biomedical applications.

## CRedit authorship contribution statement

**Noelia D. Falcon:** Data curation, Formal analysis, Investigation, Methodology, Software, Writing - original draft, Writing - review & editing. **Aram Saeed:** Conceptualization, Data curation, Formal analysis, Funding acquisition, Investigation, Methodology, Project administration, Resources, Software, Supervision, Validation, Visualization, Writing - original draft, Writing - review & editing.

## Declaration of Competing Interest

The authors declare a patent filed that related to this work by UEA Enterprises Limited (2103120.8). Aram Saeed is the sole inventor of this filed patent.

## Acknowledgements

The authors would like to thank EPSRC (EP/S021485/1) and UEA (POC192004) for their contribution toward funding this work. The authors would also like to thank PhD student Sean Tattan for contribution to revision of the manuscript and scientific discussions. We would also like to thank the project students including Chris Kirchoff, Michael Ayoub, Amy Lau, Victoria Tran, Laura Skittrall, and Aisha Shakreen for working on this project.

## Data availability

The raw/processed data required to reproduce these findings cannot be shared at this time as the data also forms part of an ongoing study and subject to patent protection.

## References

- [1] R.P. Brannigan, A.P. Dove, Synthesis, properties and biomedical applications of hydrolytically degradable materials based on aliphatic polyesters and polycarbonates, *Biomater. Sci.* 5 (1) (2017) 9–21.
- [2] B.D. Ulery, L.S. Nair, C.T. Laurencin, Biomedical Applications of Biodegradable Polymers, *J. Polym. Sci. B Polym. Phys.* 49 (12) (2011) 832–864.
- [3] I. Manavitehrani, A. Fathi, H. Badr, S. Daly, A. Negahi Shirazi, F. Dehghani, Biomedical Applications of Biodegradable Polyesters, *Polymers (Basel)* 8 (1) (2016) 20.
- [4] X. Sun, C. Xu, G. Wu, Q. Ye, C. Wang, Poly(Lactic-co-Glycolic Acid): Applications and Future Prospects for Periodontal Tissue Regeneration, *Polymers (Basel)* 9 (6) (2017) 189.
- [5] J. Wang, L. Helder, J. Shao, J.A. Jansen, M. Yang, F. Yang, Encapsulation and release of doxycycline from electrospray-generated PLGA microspheres: Effect of polymer end groups, *Int. J. Pharm.* 564 (2019) 1–9.
- [6] H.K. Makadia, S.J. Siegel, Poly Lactic-co-Glycolic Acid (PLGA) as Biodegradable Controlled Drug Delivery Carrier, *Polymers (Basel)* 3 (3) (2011) 1377–1397.
- [7] F.Y. Han, K.J. Thurecht, A.K. Whittaker, M.T. Smith, Bioerodable PLGA-Based Microparticles for Producing Sustained-Release Drug Formulations and Strategies for Improving Drug Loading, *Front. Pharmacol.* 7 (185) (2016).
- [8] Y.-P. Jiao, F.-Z. Cui, Surface modification of polyester biomaterials for tissue engineering, *Biomed. Mater.* 2 (4) (2007) R24–R37.
- [9] Y. Bu, J. Ma, J. Bei, S. Wang, Surface Modification of Aliphatic Polyester to Enhance Biocompatibility, *Front. Bioeng. Biotechnol.* 7 (2019), 98–98.
- [10] P. Gentile, V. Chiono, I. Carmagnola, P.V. Hattori, An overview of poly(lactic-co-glycolic) acid (PLGA)-based biomaterials for bone tissue engineering, *Int. J. Mol. Sci.* 15 (3) (2014) 3640–3659.
- [11] M.R. Casanova, R.L. Reis, A. Martins, N.M. Neves, Surface biofunctionalization to improve the efficacy of biomaterial substrates to be used in regenerative medicine, *Mater. Horiz.* 7 (9) (2020) 2258–2275.
- [12] H. Shen, X. Hu, F. Yang, J. Bei, S. Wang, Combining oxygen plasma treatment with anchorage of cationized gelatin for enhancing cell affinity of poly(lactide-co-glycolide), *Biomaterials* 28 (29) (2007) 4219–4230.
- [13] K.W. Chun, H.S. Yoo, J.J. Yoon, T.G. Park, Biodegradable PLGA microcarriers for injectable delivery of chondrocytes: effect of surface modification on cell attachment and function, *Biotechnol. Prog.* 20 (6) (2004) 1797–1801.
- [14] M. Rahmati, E.A. Silva, J.E. Reseland, C.A. Heyward, H.J. Haugen, Biological responses to physicochemical properties of biomaterial surface, *Chem. Soc. Rev.* 49 (15) (2020) 5178–5224.
- [15] T.I. Croll, A.J. O'Connor, G.W. Stevens, J.J. Cooper-White, Controllable surface modification of poly(lactic-co-glycolic acid) (PLGA) by hydrolysis or aminolysis I: physical, chemical, and theoretical aspects, *Biomacromolecules* 5 (2) (2004) 463–473.
- [16] Y. Zhuang, H. Shen, F. Yang, X. Wang, D. Wu, Synthesis and characterization of PLGA nanoparticle/4-arm-PEG hybrid hydrogels with controlled porous structures, *RSC Adv.* 6 (59) (2016) 53804–53812.
- [17] X. Liu, J.M. Holzwarth, P.X. Ma, Functionalized Synthetic Biodegradable Polymer Scaffolds for Tissue Engineering, *Macromol. Biosci.* 12 (7) (2012) 911–919.
- [18] H. Tan, D. Huang, L. Lao, C. Gao, RGD modified PLGA/gelatin microspheres as microcarriers for chondrocyte delivery, *J. Biomed. Mater. Res. B Appl. Biomater.* 91 (1) (2009) 228–238.
- [19] M. Alvarez-Paino, M.H. Amer, A. Nasir, V. Cuzzucoli Crucitti, J. Thorpe, L. Burroughs, D. Needham, C. Denning, M.R. Alexander, C. Alexander, Polymer Microparticles with Defined Surface Chemistry and Topography Mediate the Formation of Stem Cell Aggregates and Cardiomyocyte Function, *ACS Appl. Mater. Interfaces* 11 (38) (2019) 34560–34574.

- [20] A.O. Saeed, S. Dey, S.M. Howdle, K.J. Thurecht, C. Alexander, One-pot controlled synthesis of biodegradable and biocompatible co-polymer micelles, *J. Mater. Chem.* 19 (26) (2009) 4529–4535.
- [21] A.O. Saeed, J.P. Magnusson, E. Moradi, M. Soliman, W. Wang, S. Stolnik, K. J. Thurecht, S.M. Howdle, C. Alexander, Modular Construction of Multifunctional Bioresponsive Cell-Targeted Nanoparticles for Gene Delivery, *Bioconjug. Chem.* 22 (2) (2011) 156–168.
- [22] X. Wang, R. Berger, J.I. Ramos, T. Wang, K. Koynov, G. Liu, H.-J. Butt, S. Wu, Nanopatterns of polymer brushes for understanding protein adsorption on the nanoscale, *RSC Adv.* 4 (85) (2014) 45059–45064.
- [23] G. Walden, X. Liao, G. Riley, S. Donell, M.J. Raxworthy, A. Saeed, Synthesis and Fabrication of Surface-Active Microparticles Using a Membrane Emulsion Technique and Conjugation of Model Protein via Strain-Promoted Azide-Alkyne Click Chemistry in Physiological Conditions, *Bioconjug. Chem.* 30 (3) (2019) 531–535.
- [24] P. van de Wetering, E.E. Moret, N.M. Schuurmans-Nieuwenbroek, M.J. van Steenberg, W.E. Hennink, Structure-activity relationships of water-soluble cationic methacrylate/methacrylamide polymers for nonviral gene delivery, *Bioconjug. Chem.* 10 (4) (1999) 589–597.
- [25] X. Liao, G. Walden, N.D. Falcon, S. Donell, M.J. Raxworthy, M. Wormstone, G. P. Riley, A. Saeed, A direct comparison of linear and star-shaped poly (dimethylaminoethyl acrylate) polymers for polyplexation with DNA and cytotoxicity in cultured cell lines, *Eur. Polym. J.* 87 (2017) 458–467.
- [26] S.K. Samal, M. Dash, S. Van Vlierberghe, D.L. Kaplan, E. Chiellini, C. van Blitterswijk, L. Moroni, P. Dubruel, Cationic polymers and their therapeutic potential, *Chem. Soc. Rev.* 41 (21) (2012) 7147–7194.
- [27] Q. Chen, D. Zhang, W. Zhang, H. Zhang, J. Zou, M. Chen, J. Li, Y. Yuan, R. Liu, Dual mechanism  $\beta$ -amino acid polymers promoting cell adhesion, *Nat. Commun.* 12 (1) (2021) 562.
- [28] E. Vey, C. Rodger, L. Meehan, J. Booth, M. Claybourn, A.F. Miller, A. Saiani, The impact of chemical composition on the degradation kinetics of poly(lactic-co-glycolic) acid copolymers cast films in phosphate buffer solution, *Polym. Degrad. Stab.* 97 (3) (2012) 358–365.
- [29] Q.A. Rafiq, K. Coopman, A.W. Nienow, C.J. Hewitt, Systematic microcarrier screening and agitated culture conditions improves human mesenchymal stem cell yield in bioreactors, *Biotechnol. J.* 11 (4) (2016) 473–486.
- [30] M.H. Rahaman, Tsuji, Hideto, Hydrolytic degradation behavior of stereo multiblock and diblock poly(lactic acid)s: Effects of block lengths, *Polym. Degrad. Stab.* 98 (3) (2013) 709–719.
- [31] T.W. Steele, C.L. Huang, S. Kumar, A. Iskandar, A. Baoxin, F.Y.C. Boey, J.S. Loo, S. S. Venkatraman, Tuning drug release in polyester thin films: terminal end-groups determine specific rates of additive-free controlled drug release, *NPG Asia Mater.* 5 (4) (2013) e46–e46.
- [32] L.N. Woodard, M.A. Grunlan, Hydrolytic Degradation and Erosion of Polyester Biomaterials, *ACS Macro Lett.* 7 (8) (2018) 976–982.